

The physical perspective on the solid and molten states associated with the mechanical properties of eco-friendly HDPE/*Pinus taeda* wood-plastic composites

Karine Grison,¹ Vinicius Pistor,² Lisete Cristine Scienza,² Ademir José Zattera¹

¹University of Caxias Do Sul - UCS/Post-graduate Program in Processes and Technology Engineering, Caxias Do Sul - RS, Brazil

²Federal University of Rio Grande Do Sul - UFRGS/Porto Alegre - RS, 91501-970, Brazil

Correspondence to: A. J. Zattera (E-mail: ajzatter@ucs.br)

ABSTRACT: The manufacture of wood plastic composites (WPCs) by reutilizing post-consumed polymeric materials and post-industry wood wastes contributes to reduce the environmental impact and the consumption of virgin plastics. In this work, the influence of interfacial adhesion on the solid and molten states of high density polyethylene (HDPE) containing WPCs wood dust of recycled *Pinus taeda* (PT) was evaluated. The composites were prepared by extrusion in a twin screw extruder using maleic anhydride as compatibilizer. The samples were analyzed by dynamic-mechanical analysis (DMA), tensile and impact strength measurements, oscillatory rheometry, differential scanning calorimetry (DSC) and scanning electron microscopy (SEM). DMA analysis showed increase in module and an improved interface with physical interaction between the WPCs phases. The higher molecular interactivity interface improved the mechanical properties relative to pure HDPE. Melting state analysis showed increased WPCs flow restriction, this feature being correlated with reduction in the molecular degree of freedom during flow, which consequently reduces the crystalline degree changes in microstructure as well as in processing parameters of the material. These results lead to consider the development of an eco-friendly and economic effective technology to reuse abundant recycled solid wastes in a new market. © 2015 Wiley Periodicals, Inc. *J. Appl. Polym. Sci.* **2016**, *133*, 42887.

KEYWORDS: cellulose and other wood products; differential scanning calorimetry; recycling; rheology; thermoplastics

Received 1 July 2015; accepted 28 August 2015

DOI: 10.1002/app.42887

INTRODUCTION

The development of ecological appeal wood plastic composites (WPCs) has been evaluated to replace traditional materials applied, e.g., in concrete manufacturing, replacement of wooden furniture, automotive industry and civil construction.^{1,2} The preparation of WPCs is important since thermoplastics are a major component of municipal solid waste. Among the polymers useful for the manufacture of these composites, polypropylene (PP), higher density polyethylene (HDPE) and polyvinyl chloride (PVC) are the most commonly investigated.^{3,4} When wood flour is used as filler, the influence of its constituents and the wood species must be considered as regards mechanical properties, as well as thermal and photochemical (color and chemical modifications) degradation of the resulting composites.^{5,6} When using nonpolar polymers (hydrophobic character) and polar components (of hydrophilic character), the interaction interface can be improved by the use of compatibilizing agents.² Maleic anhydride is able to promote such interaction at low percent of incorporation (2% by weight) while improving the composite mechanical

(flexural and impact) properties.⁷ In general, the addition of 1–3 wt %, based on the total weight of composites of maleic anhydride is able to improve the mechanical properties.⁸ Studies have shown that the addition of up to 50% eucalyptus powder into low density polyethylene (LDPE) compatibilized with maleic anhydride was able to improve the mechanical strength of the composite.⁹ The WPCs final properties are important to impart reliability in the use of artifacts with recycled materials even if the ecological appeal is currently interesting. In order to improve the balance of properties, adhesion control is a question addressed in several studies^{7,10} since high percentages of filler can also change the processing conditions of the material. In this work the influence of the interfacial adhesion on the solid and molten states and on the physical properties of wood-plastic composites based on high density polyethylene (HDPE) and wood dust of recycled *Pinus taeda* (PT) was evaluated.

MATERIALS

For blow extrusion, HDPE (ES-6004) homopolymer supplied by Braskem (SP/Brazil) with melting flow index of 0.35 g/10 min

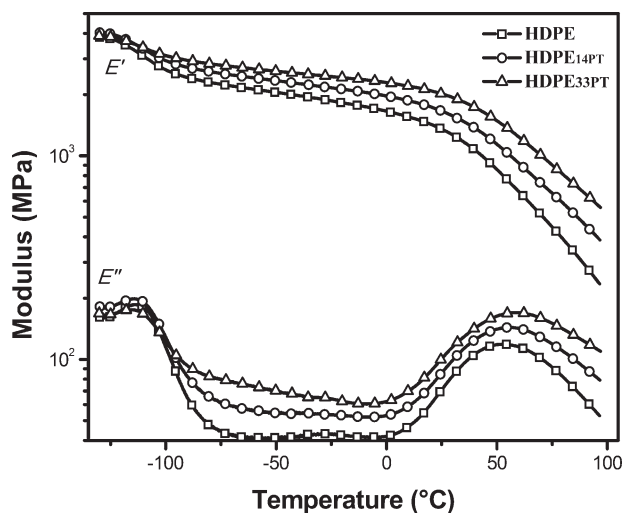


Figure 1. DMA curves illustrating the modulus values obtained for HDPE and the PT-containing composites.

(measured at 190°C with load of 16 kg), was used. (Polyethylene-co-maleic anhydride (MA) (Polybond 3029) ($T_m = 130^\circ\text{C}$, density = 0.95 g/cm^3 and MA content of $\approx 1.5\text{--}1.7\%$) supplied by Chemtura Industry was used as compatibilizing agent and PT wood was supplied by a branch company of building materials of Caxias do Sul-Brazil.

METHODS

Sample Preparation

The PT wood was ground in a two-knife mill, at first using a Primotécnica, model 1001 mill, and afterwards using a Marconi, model MA580 mill to obtain smaller particles. The granulometric distribution was classified using a particle size classifier (Prodest) of 35, 48, 65, 100, and 150 mesh sieves. Based on the literature, the particle size was between 65 and 100 mesh.¹¹ The PT powder was dried in an oven with air circulation at 80°C for 24 h. Samples were prepared by the melt mixing process in a corotating interpenetrating twin-screw extruder (MH-COR-20-32-LAB, MH Equipamentos; $D = 20\text{ mm}$, $L/D = 32$). Eight heating zones and temperature profiles of 145, 170, 180, 180, 178, 165, 180, and 185°C , respectively, and a speed rotation of 200 rpm were used with the aid of a vacuum degassing (zone 5*). Between 14 and 33% by weight of PT wood flour and 2% by weight of MA was added.

Characterization

The viscoelastic properties were determined with a TA Instruments Dynamic Mechanical Analyzer (DMA) Q800. Tests were performed at the frequency of 1 Hz and heated from -130 to 100°C using a heating rate of $3^\circ\text{C}/\text{min}$, the analysis being carried out at single cantilever mode and strain amplitude of 1%.

The samples were analyzed in an Anton Paar oscillatory rheometer (Physica MCR 101), with parallel plates of 25 mm diameter and spacing between the plates of 1 mm, test temperature of 190°C , in the range of 0.1 and 100 Hz, test stress maximum of 200 Pa and nitrogen flow of $1\text{ m}^3/\text{h}$.

Tensile strength tests were performed according to ASTM D 638:10 Method at 10 mm/min using a universal testing machine EMIC DL 2000. IZOD impact test with notch, pendulum of 1 J and speed of 3.5 m/s using CEAST (Resil 25) was performed in agreement with the ASTM D 256:10 Method.

DSC (DSC50 – Shimadzu) analysis was performed under N_2 atmosphere (50 ml/min) using approximately 10 mg of each sample. The samples were initially heated from ambient temperature ($\approx 25^\circ\text{C}$) to 200°C and then cooled to -40°C and heated again to 200°C , both steps being performed at a heating rate of $10^\circ\text{C}/\text{min}$.

SEM analysis was carried out using a Superscan S-550 apparatus, with a secondary electron detector and acceleration voltage of 15.0 kV. The samples were previously metalized with gold.

RESULTS AND DISCUSSION

Figure 1 shows the storage (E') and loss (E'') moduli for HDPE and the composites studied. Two ranges of transition can be seen through the temperature monitored. Thus, near -110°C the β transition (T_β) was observed for the samples. This transition is characteristic of branched materials however, its presence in the case of HDPE may be correlated with material fractions on the crystalline interface that are partially ordered, i.e., the presence of T_β is evident when interfaces between crystals are composed of up to 10% of the microstructure.¹² Comparatively, there was no significant evidence of variations in T_β for the composites, this being probably due to its narrow range of measurement as compared to the more large transitions observed for the α transition (T_α).

T_α was observed between 0 and 100°C , being correlated with the crystalline degree¹³ and being also dependent on the average crystal thickness.^{12,14} It is also described as a transition arising from short-range rotational motions in molecular structures and its amplitude of variation is considered lower than the glass transition.¹⁵ In the vitreous plateau ($\approx -75\text{--}0^\circ\text{C}$) and in T_α values observed in Figure 2, through the $\tan \delta$ curves, the

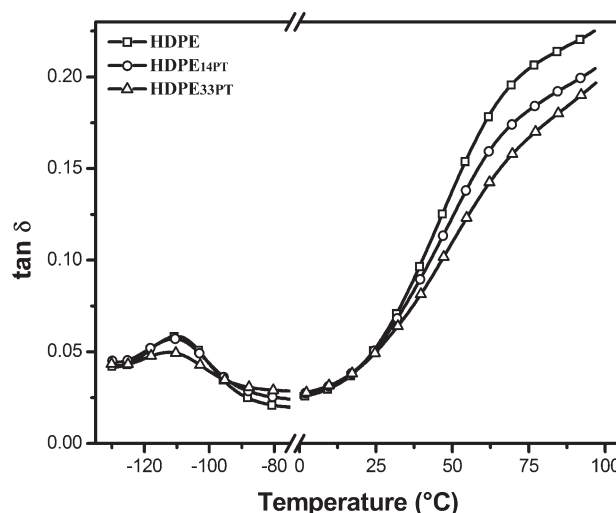


Figure 2. $\tan \delta$ curves obtained by the E''/E' relationship for HDPE and the composites studied.

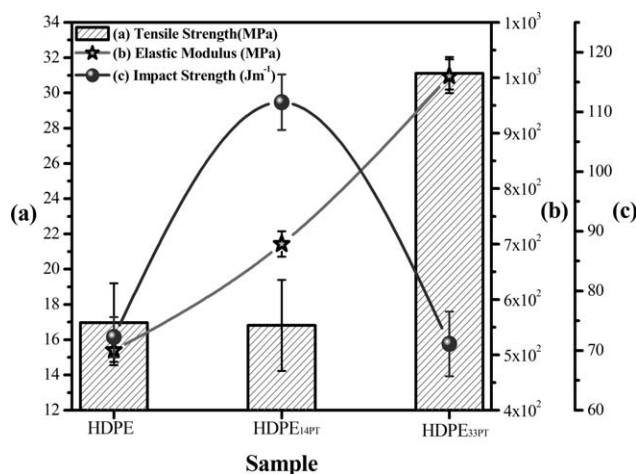


Figure 3. Mechanical properties, where: axes (a) and (b) are the tensile strength and elastic modulus, respectively obtained by tensile strength tests and axis (c) is the impact strength analysis.

composites showed increased modulus proportional to the *PT* addition, as compared to HDPE. The increment in modulus in the vitreous plateau suggests a reinforcement effect by the filler probably due to the increased thermal energy of the molecular movements between the amorphous and crystalline regions.¹⁶ On the vitreous plateau there are no crystal motions and the reinforcement effect is probably due to the ability of the filler to hinder the degree of freedom on crystal interfaces at ranges of motion before the onset of the T_x .

The T_x values for the composites not were changed; however, there was a reduction in the T_β height intensity for the HDPE_{33PT} composite. This change in T_β suggests that the higher amount of *PT* wood flour was capable to promote deeper molecular interactivity between crystals and hinder the energy dissipation on their interface. Figure 3 illustrates the mechanical response of the addition of *PT* wood flour into HDPE.

The tensile strength (σ) [axis (a)] was increased only for the 33 wt % *PT* sample, however the elastic modulus (E) [axis (b)]

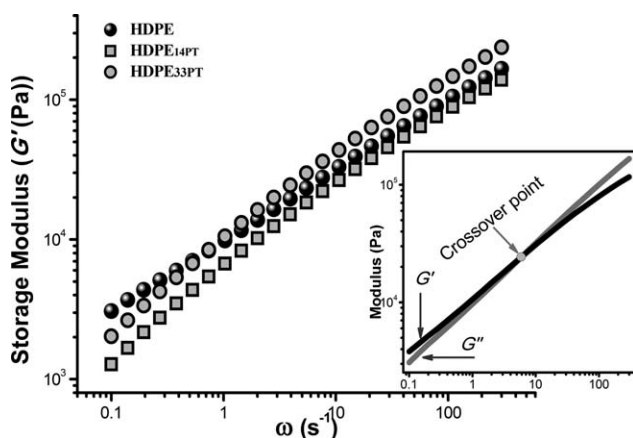


Figure 4. Analysis of oscillatory rheometry, where: (a) is the storage modulus (G') and (b) the crossover point between G' and the loss modulus (G'') illustrated for HDPE.

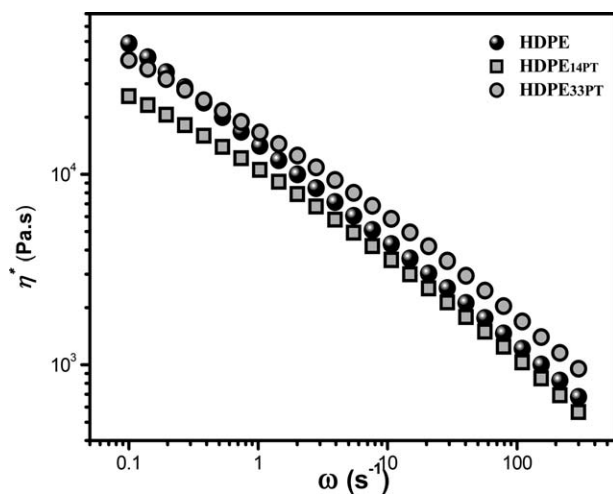


Figure 5. Complex viscosity (η^*) obtained from oscillatory rheometry analysis.

increased progressively for 14 and 33 wt % *PT*. The higher E for the HDPE_{33PT} sample supports the more interactive action on T_β . Moreover, the addition of 14 wt % *PT* showed a 54% increase in impact strength [axis (c)] correlated only with the increase in σ since for this sample the E values were not changed. For the 33 wt % *PT* the impact strength probably did not change since the reinforcement restricts the dissipation of energy making the rigid structure unable to support mechanical stress by excess filler.

The upper limit of addition of this wood suggests a setback in this property, considering the average particle diameter used. Nevertheless, from the viewpoint of compatibility the interaction effectiveness is noted by the increase in E . Literature results show that the incorporation of 30 wt % of wood fiber generates increment in the HDPE mechanical properties;¹⁷ however, in other researches the incorporation of up to 40 wt %¹⁸ and 50 wt %¹⁹ of wood powder, e.g., into a PP matrix, promoted

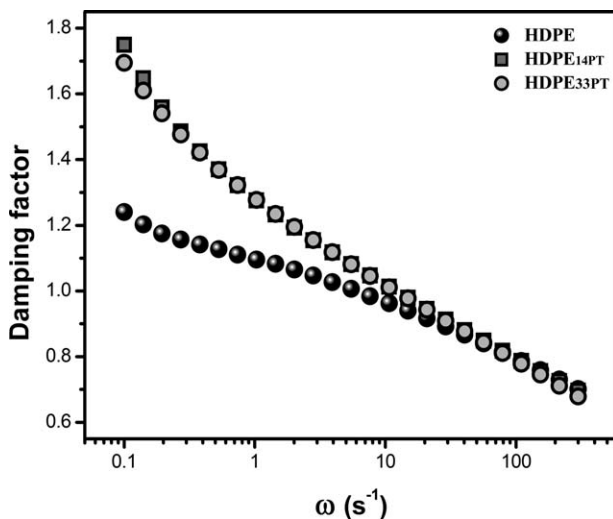


Figure 6. Damping factor curves obtained by oscillatory rheometry for HDPE and the *PT*-containing composites.

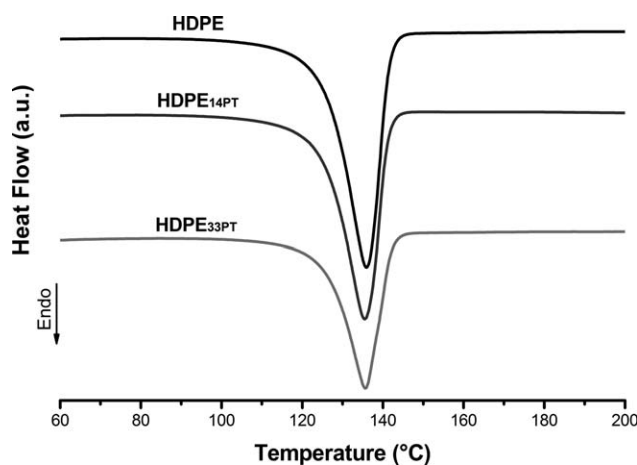


Figure 7. DSC thermograms obtained for neat HDPE and the *PT*-containing composites.

increment in E values and increase in the σ and impact strength, respectively. Moreover, also the addition of 40 wt % of, e.g., viscose fiber into HDPE showed increment in σ and E values.²⁰ In most cases, the improvement in mechanical properties can be attributed to factors such as aspect ratio of the fiber, average particle size, compatibilizing agent, method of mixture and other factors. Figure 4(a) shows the storage modulus (G') as a function of the angular frequency (ω) in the melting state and Figure 4(b) shows the storage modulus G' and the loss modulus (G'') to illustrate the HDPE crossover point.

From the higher ω , the G' tends to increase since there are lower intervals of molecular relaxation. The short molecular motion tends to present a solid elastic behavior.²¹ For the HDPE_{14PT} composite at lower ω values, $\approx 0.1 - 1 \text{ s}^{-1}$, G' value was lower than that of neat HDPE. The decrease in G' may be due to the fact that the addition of *PT* wood flour favors chains motion during the moving of the molten material. At higher ω , the G' values are close to those of HDPE. At lower ω the HDPE_{33PT} sample showed G' values intermediary to those of HDPE and HDPE_{14PT} and, with the increase in frequency ($\omega > 1 \text{ s}^{-1}$) tended to higher values than those observed for neat HDPE. As illustrated in Figure 4(b) from the representation of the crossover point between G' and G'' , the estimated values were $24 \times 10^3 \text{ Pa}$, $28 \times 10^3 \text{ Pa}$ and $46 \times 10^3 \text{ Pa}$ for neat HDPE, HDPE_{14PT} and HDPE_{33PT}, respectively. The ω values in the crossover point were 6 s^{-1} for HDPE and 12 s^{-1} for HDPE_{14PT} and HDPE_{33PT}. The crossover is the point where the molecular disentanglement and the chains are free to slide over each other. The higher value at the crossover point, mainly for

the HDPE_{33PT} sample, suggests that the *PT*-containing sample was able to hinder the flow generating spatial resistance during the sliding of chains. This restriction behavior reflects on the complex viscosity (η^*) as illustrated in Figure 5. The complex viscosity (η^*) behavior of the HDPE_{14PT} sample was close to that of neat HDPE and showed lower viscosity at low ω , which corroborates the G' arguments. At higher ω the η^* value was also close to that of HDPE. For the HDPE_{33PT} sample, from the crossover point increased η^* was observed, as compared to the other samples, and this increase corroborates the restrictive effect during the HDPE flow.

Figure 6 shows the damping factor curves obtained by the ratio between moduli in oscillatory rheometry data (G''/G'). These curves are able to evaluate the interfacial behavior between the composite components under the viewpoint of molecular interaction. The damping factor lower values are associated with the lower interactive interface of the components.²² When the viscous and elastic portions are in equilibrium during flow, $G''/G' \approx 1$ (correlated with the crossover point); however, when the viscous component (dissipative factor) is higher, $G''/G' < 1$ whereas when it is the elastic component which is higher, $G''/G' > 1$ and energy conservation predominates.²³

At low ω the damping factor of both composites was higher than that of neat HDPE suggesting that for larger molecular relaxation times, *PT* addition causes restrictions to molecular degrees of freedom, hindering the flow behavior. This restriction to flow decreases with the increase in ω leading to values close to those of neat HDPE and this occurs because higher ω does not favor the *PT* interaction along the diffusion of chains in the flow. The DSC thermograms are illustrated in Figure 7 and the parameters obtained by the first and second heating are shown in Table I. The melting point temperature (T_m) observed in the thermograms and Table I for the second heating remained constant for all samples ($\approx 135^\circ\text{C}$). For neat HDPE, the typical T_m value is 130°C .¹⁰ The percentage of crystallinity was estimated using as heat of fusion 295.8 J/g .²⁴

For the first heating the T_m values were all $\approx 132^\circ\text{C}$. The difference in T_m values between the first and second heating while not being significant, may be related to the presence of structural stresses associated with crystallization kinetics during processing. The perturbation in crystallization kinetics could be seen through the melting enthalpy values (ΔH_m) and crystallinity degree (X_c) which were lower for the first heating than for the second one. For both heating steps, *PT* addition decreased the HDPE ΔH_m and X_c values according to the amount of filler. This decrease is probably due to a trans-crystallization mechanism where the nucleation point occurs on the surface of the

Table I. DSC Parameters Obtained from Thermograms of First and Second Heating for Neat HDPE and the WPCs

Amostra	First heating			Second heating		
	ΔH_m (J/g)	T_m ($^\circ\text{C}$)	X_c (%)	ΔH_m (J/g)	T_m ($^\circ\text{C}$)	X_c (%)
HDPE	183	133	62	197	136	67
HDPE _{14PT}	166	132	57	180	135	61
HDPE _{33PT}	117	133	40	129	135	44

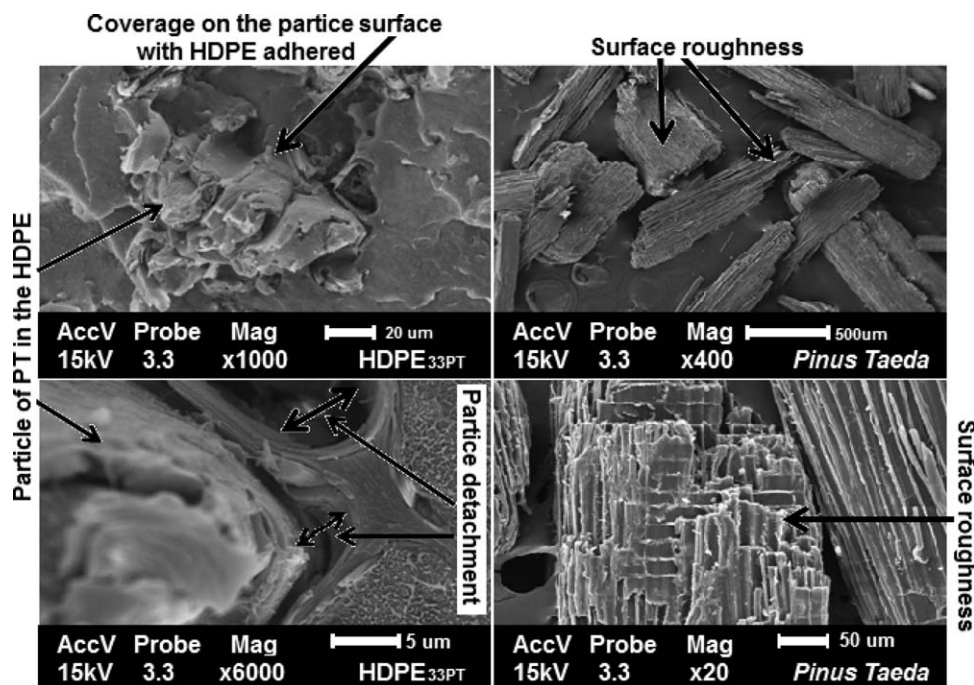


Figure 8. MEV Images comparing the individual particles of *PT* (right images) and the fractured surface of the composite containing 33 wt % of *PT* into the HDPE matrix (left images).

particles affecting the kinetics of crystallization and favors the smaller, heterogeneous crystal formation.²⁵

The reduction in the heat absorbed by the melting crystals suggests that the loss of crystals structural integrity is probably favored by the filler on the crystals interfaces. This evidence is supported mainly for the HDPE_{33PT} composite that showed the reduced T_{β} intensity observed in Figure 2 and the decrease in G' at low ω (Figure 1). Wood as filler can result in variations in melting and slower crystallization rate according to its content, as well as the geometry and compatibility of the filler.²⁶ Moreover, the easier melting does not necessarily mean that the composites are more mechanically fragile or susceptible to lose the macroscopic properties, as seen by the mechanical properties (Figure 3). The decrease in size of the crystalline domains and the adhesion between *PT* and HDPE through the compatibilizing agent may contribute to the more favorable energy dissipation mechanism due to the higher concentration of dispersive regions in the microstructure. The interface improvement between *PT* and HDPE can be seen by the increased E values (Figure 3) and the higher damping factor (Figure 6). Figure 8 shows MEV images of the HDPE_{33PT} composite (obtained on the fractured surface during impact resistance analysis) and the *PT* particles.

The *PT* surface is composed of irregularities, which generate a roughened surface along all particles. This roughness is important because it enables the melting polymer to use the particle surface as anchoring point, favoring adhesion during the crystallization process. As can be observed in the HDPE_{33PT} composite images, the *PT* particles did not have the same roughness as the individual particles. This difference may be associated to the fact that the HDPE particles are adhered on the *PT* surface, the adhesion being favored by the surface roughness of the

particle. However, this surface irregularity generates perturbations in the homogeneity of the crystals decreasing the enthalpy and the HDPE crystalline degree.

CONCLUSIONS

Recycled *PT* wood dust was used to manufacture wood-plastic composites with high density polyethylene (HDPE) by mixing the components in a twin screw extruder using maleic anhydride as compatibilizing agent. DMA analysis demonstrated that the preferential *PT* interaction occurs on the interface between the crystalline and amorphous phases and hinder the movements correlated with the HDPE interlamellar amorphous fractions. The increased storage modulus and the reduction in the $\tan \delta$ value suggested that the *PT* acts as reinforcement and promotes higher molecular cooperation on the microstructure. The higher molecular interactivity favors the progressive increase in the elastic modulus as determined by tensile strength analysis and also increases the impact strength for the *PT* lower content. The impact strength did not increase for the higher *PT* content suggesting that there is a limit for its addition aiming at the tenacity increases in parallel with the modulus. Oscillatory rheometry data showed that *PT* addition, mainly for the higher content, hinders the molecular disentanglement effects in the melting state for higher frequencies. This behavior can promote changes in the flow behavior and in the processing conditions of the industrial manufacture. The *PT* addition decreased the melting enthalpy and the crystalline degree of the composites demonstrating that the flow effects are correlated with the interaction among the composites phases. Through MEV images, it was possible to observe polymer adhesion on the *PT* surface, which may be favored by the surface roughness of the particle and further by the compatibilizing agent. This adhesion is

probably responsible for the effects associated with crystallinity modification.

ACKNOWLEDGMENTS

The authors gratefully acknowledge UCS, CAPES, and CNPq for providing scholarships and financial support.

REFERENCES

1. Dittenber, D. B.; Rao, H. V. S. G. *Compos. A* **2012**, *43*, 1419.
2. Valente, M.; Sarasini, F.; Marra, F.; Tirillo, J.; Pulci, G. *Compos. A* **2011**, *42*, 649.
3. Monteiro, S. N.; Calado, V.; Rodriguez, R. J.; Margem, F. M. *Mater. Sci. Eng. A* **2012**, *557*, 17.
4. Ndiaye, D.; Fanton, E.; Morlat-Therias, S.; Vidal, L.; Tidjani, A.; Gardette, J. L. *Compos. Sci. Technol.* **2008**, *68*, 2779.
5. Zabihzadeh, M.; Ebrahimi, G.; Dastoorian, F. *J. Reinforced Plast. Compos.* **2009**, *29*, 1146.
6. Fabiyi, J. S.; Mcdonald, A. G. *Compos. Part A* **2010**, *41*, 1434.
7. Poletto, M.; Dettenborn, J.; Zeni, M.; Zattera, A. J. *Waste Manage.* **2011**, *31*, 779.
8. Lu, J. Z.; Wu, Q.; Mcnabb, J. R. H. S. *Wood Fiber Sci.* **2000**, *32*, 88.
9. Redighieri, K. I.; Costa, D. A. *Polímeros: Ciência E Tecnologia* **2008**, *18*, 5.
10. Najafi, S. K. *Waste Manage.* **2013**, *33*, 1898.
11. Poletto, M.; Zeni, M.; Zattera, A. J. *J. Thermoplast. Compos. Mater.* **2012**, *25*, 821.
12. Popli, R.; Glotin, M.; Mandelkern, L.; Benson, R. S. *J. Polym. Sci. Part B: Polym. Phys.* **1984**, *22*, 407.
13. Ashcraft, C. R.; Boyd, R. H. *J. Polym. Sci. Polym. Phys.* **1976**, *14*, 2153.
14. Alberola, N.; Cavaille, J. Y.; Perez, J. *Polym. Sci. Part B: Polym. Phys.* **1990**, *28*, 569.
15. McCrum, N. G.; Read, B. E.; Williams, G. *Anelastic and Dielectric Effects in Polymeric Solids*; New York: Wiley, **1965**.
16. Sewda, K.; Maiti, S. N. *Polym. Bull.* **2013**, *70*, 2657.
17. Peltola, H.; Pääkkönen, E.; Jetsu, P.; Heinemann, S. *Compos. Part A: Appl. Sci. Manufact.* **2014**, *61*, 13.
18. Diaz, C. A.; Afrifah, K. A.; Jin, S.; Matuana, L. M. *Compos. Sci. Technol.* **2011**, *71*, 67.
19. Sobczak, L.; Lang, R. W.; Haider, A. *Compos. Sci. Technol.* **2012**, *72*, 550.
20. Pöllänen, M.; Suvanto, M.; Pakkanen, T. T. *Compos. Sci. Technol.* **2013**, *76*, 21.
21. Ferry, J. D. *Viscoelastic Properties of Polymers*, 3rd ed. New York: John Wiley & Sons, **1980**.
22. Pistor, V.; Lizot, A.; Fiorio, R.; Zattera, A. J. *Polymer* **2010**, *51*, 5165.
23. Hyun, Y. H.; Lim, S. T.; Choi, H. J. J. H. O. N.; M. S. *Macromolecules* **2001**, *34*, 8084.
24. Sánchez-Soto, M.; Rossa, A.; Sánchez, A. J.; Gámez-Pérez, J. *Waste Manage.* **2008**, *28*, 2565.
25. Guo, B.; Yang, M.; Tan, J.; Zhang, H.; Fu, Q. Q. *Polym. Int.* **2006**, *55*, 441.
26. Cui, Y. H.; Tao, J.; Noruziaan, B.; Cheung, M.; Lee, S. J. *J. Reinforced Plast. Compos.* **2010**, *29*, 278.